Anuário do Instituto de Geociências
Universidade Federal do Rio de Janeiro
https://revistas.ufrj.br/index.php/aigeo/

ISSN 0101-9759
e-ISSN 1982-3908

Spatial Analysis of the Impacts Caused by Changes in Land Use on the Estimation of Surface Temperature in the The City of Paracatu (MG)

Análise Espacial dos Impactos Ocasionados pelas Mudanças no Uso da Terra na Estimativa da Temperatura Superficial da Cidade de Paracatu (MG)

Arthur Pereira dos Santos & Henzo Henrique Simionatto

Universidade Estadual Paulista, Instituto de Ciência e Tecnologia, Sorocaba, SP, Brasil
E-mails: arthur.p.santos@unesp.br; henzo.h.simionatto@unesp.br

Abstract

The increase in built-up areas, coupled with the suppression of vegetation without the necessary mitigating measures to curb the effects of urbanization, causes changes in the microclimate and directly impacts the health of the local population. In this sense, the present study aims to analyze the influence of land cover type on the variation of Land Surface Temperature (LST) estimation in the city of Paracatu, Minas Gerais (MG), in the years 1990 and 2020.For this, the maps provided by the Annual Mapping of Land Cover and Land Use of Brazil (MapBiomas) and images from the LANDSAT-5 (1990) and LANDSAT-8 (2020) satellites were used. Four images, distributed across seasons, were utilized to estimate LST for these periods, aiming to obtain a representative LST estimate for that year. For the calculation of the LST with bands 6 and 10, respectively of the LANDSAT-5 and 8 satellites, the SCP plugin of the QGIS software was used, and the process of recovery of the LST in the scenes used occurred through conversion of the values of the Digital Number (DN) into radiance at the Top of the Atmosphere (ToA), conversion of radiance into brightness temperature in ToA, correction of atmospheric effects and obtaining LST in Kelvin and, subsequently, in degrees Celsius. After that, the average between them was performed by means of normalization of each of the scenes, obtaining a representative mosaic for the LST of each year,thus enabling the estimation of the spatial behavior of the minimum, mean, and maximum values.. Finally, in order to verify the influence of Changes in Use and Occupation (LULC) on the spatial variation of the LST, the classes found in Vegetation, Exposed Soil, Urban Area and Water Resources were segmented, and it was found that, while the urban area of Paracatu had its territorial extension practically doubled, the vegetation class decreased by almost 25%, a fact that implied in the average increase of the LST by more than 5º C. the minimum and maximum values of these classes varied around 4.5 and 3º C, and it is possible to conclude that, in this interval of 30 years, Paracatu had no urban growth occurring exponentially and without the proper mitigations for the transformation of the microclimate, implying the need for measures that can curb these changes in strategic points of the municipality, as in the Bom Pastor neighborhood, which had its use and occupation totally changed in this temporal hiatus. In addition, in view of the estimates of economic growth in the city, it is believed that these measures should be taken as a matter of urgency, so that the results presented here can support the decisions of the managing public agencies.

Keywords: Urban climate; Remote sensing; Territorial management

Resumo

O incremento das áreas construídas, atrelado à supressão da vegetação sem as medidas mitigadoras necessárias para frear os efeitos da urbanização, ocasionam em alterações no microclima e impactam diretamente a saúde da população local. Nesse sentido, o presente trabalho objetiva analisar a influência do tipo de cobertura da terra na variação da estimativa da temperatura da superfície - *Land Surface Temperature* (LST) - da cidade de Paracatu, Minas Gerais (MG) nos anos 1990 e 2020. Para isso, utilizou-se os mapas disponibilizados pelo Mapeamento Anual da Cobertura e Uso do Solo do Brasil (MapBiomas) e imagens dos satélites LANDSAT-5 (1990) e LANDSAT-8 (2020). Foram utilizadas 4 imagens, distribuídas por estações do ano, para estimar a LST desses períodos, visando obter uma estimativa da LST representativa para aquele ano. Para o cálculo da LST com as bandas 6 e 10, respectivamente dos satélites LANDSAT-5 e 8, utilizou-se o plugin SCP do software QGIS, e o processo de recuperação da LST nas cenas utilizadas ocorreu por meio de conversão dos valores do Número Digital (DN) em radiância no Topo da Atmosfera (ToA), conversão de radiância em temperatura de brilho no ToA, correção dos efeitos atmosféricos e obtenção da LST em Kelvin e, posteriormente, em graus Celsius. Após isso, realizou-se a média entre essas por meio de normalização de cada uma das cenas, obtendo um mosaico representativo para a

Received: 26 October 2022; Accepted: 23 July 2024
Anu. Inst. Geociên., 2024;47:55194 DOI: https://doi.org/10.11137/1982-3908_2024_47_55194

LST de cada ano, sendo possível, dessa forma, estimar o comportamento espacial dos valores mínimos, médios e máximos. Por último, para verificar a influência das Mudanças de Uso e Ocupação (LULC) na variação espacial dessa estimativa LST, segmentou-se as classes encontradas em Vegetação, Solo Exposto, Área urbana e Recursos Hídricos, constatando-se que, enquanto a área urbana de Paracatu teve a sua extensão territorial praticamente dobrada, a classe de vegetação diminuiu em quase 25%, fato que implicou no aumento médio da LST em mais de 5º C. Além do mais, os valores mínimos e máximos dessas classes chegaram a variar em torno de 4.5 e 3º C, sendo possível concluir que, nesse intervalo de 30 anos, Paracatu teve seu crescimento urbano ocorrido de forma exponencial e sem as devidas mitigações para transformação do microclima, implicando na necessidade de medidas que possam frear essas alterações em pontos estratégicos do município, como no bairro Bom Pastor, que teve seu uso e ocupação totalmente alterado nesse hiato temporal. Além do mais, diante das estimativas de crescimento econômico na cidade, acredita-se que essas providências devam ser tomadas em caráter de urgência, de forma que os resultados aqui apresentados possam subsidiar as decisões dos órgãos públicos gestores.

Palavras-chave: Clima urbano; Sensoriamento remoto; Gestão territorial

1 Introduction

In the 20th century, urbanization in the world increased exponentially, especially in developing countries (Nagendra et al., 2018). Because it happened in an unplanned way, a series of uncertainties came to the fore, as well as several discussions about future projections (Jiang & O'Neill, 2017), as adaptations and coping with population growth in relation to climate change, urbanization rate and water resources that are within cities (Zhang et al., 2020).

Although currently less than 3% of land areas are considered urban, cities are home to most of the world's population, and their expansion is the most evident form of transformation of the natural landscape, directly affecting the microclimate (Santos and Simionatto, 2023), which is defined as urban climate (Monteiro 1997).

United Nations Organization (ONU) estimates that, by 2050, the urbanization rate in Brazil will rise from 87 to 92% (ONU 2019). The relationship between rural and urban population has changed significantly in the country during the last century. Zago (2016) mentions that less than 20% of the population lives in rural areas. By presenting an urbanization model characterized by unbridled and unplanned growth, Brazilian cities grew with numerous vulnerable areas, socially and environmentally.

With changes in the use and occupation of cities, variations in LST also occurred. In this way, efficient urban management becomes a pressing challenge for the executive branch (Saha et al., 2021), because the increase in LST for anthropic reasons of LULC is currently one of the most critical urban climate effects (Steeneveld et al. 2018; Kafy et al. 2022).

Thus, as much as changes in the thermal climate of cities are inevitable, mitigating measures need to be taken so that the effects of the formation of Urban Heat Islands (UHI) are minimized (Vandamme et al. 2019), because, in areas with heterogeneous surface patterns, such as urban areas, the decrease in bioclimatic comfort is practically inevitable (Lopes et al., 2022).

The study of LULC and its impacts on LST variation has become an important subject in urban planning and land management research, as well as urban meteorology, ecology and geography. For future adoption of sustainable adaptation measures, better information and knowledge are needed about the magnitude of LST caused by urban sprawl, especially in cities in constant economic and population development (Sresto et al. 2022).

This is the case of the municipality of Paracatu (MG), historical center of the northwest mesoregion of MG and national prominence in mineral production and agriculture, directly causing an intense migratory flow, which has been impacting the average annual population growth of the city (Santos et al. 2021), corroborating the need for studies that, like this one, can support public bodies in decision-making that address the use and occupation of the municipality's land, because, so far, nothing is known about the interference of anthropic occupation on changes in the urban microclimate.

In view of the increase in impermeable surfaces and built-up areas in the municipality, one of the growing and viable opportunities, through SR techniques, is that of studies that can evaluate the impacts of the space-time dynamics of the LULC on the variability of the LST (Ismail et al. 2021).Thus, the present study aims to analyze, in an interval of 30 years, the LULC of the urban mesh of Paracatu and the influence that such changes caused in the estimation of LST.

2 Materials and Methods

2.1 Study Area

Located 220 km from the federal capital, Brasília - Distrito Federal (DF), Paracatu - MG (Figure 1), it belongs entirely to the cerrado biome, being a national highlight in tourism, mineral wealth, agribusiness, and agriculture, a fact that has been impacting its economic growth and, consequently, its population variation (Santos et al. 2022b).

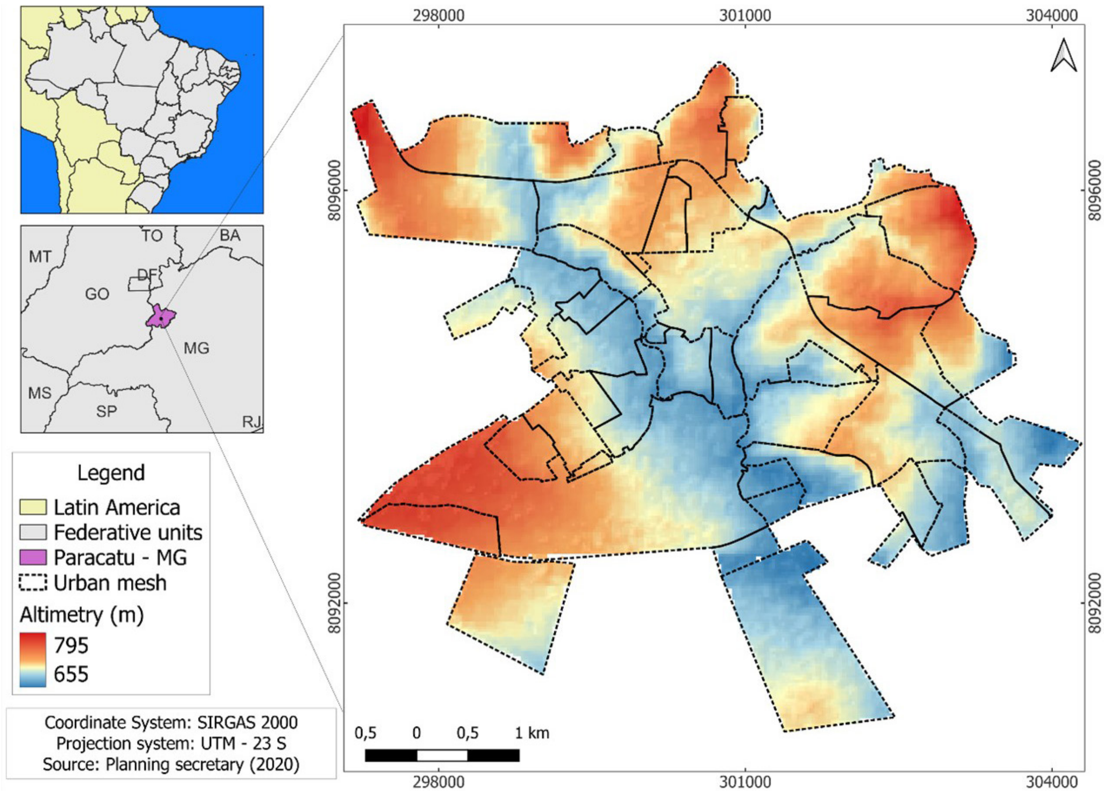

Figure 1 Study area.

In 1990, the population of Paracatu totaled approximately 62.700 inhabitants, while in 2020 the municipality was occupied by approximately 92.000 people, according to population estimates by the Brazilian Institute of Geography and Statistics (IBGE) for these periods (IBGE 1991; IBGE 2020). Currently, Paracatu has a population of approximately 94.000 people (IBGE 2022).

The climate of the municipality is humid tropical savannah, with dry winters and rainy summers, type Aw, according to the Köppen classification, and its average annual temperature is 22.6 ºC. The average rainfall is 1,450 mm/year and its altitude is between 500 and 950 meters (INMET 2020). According to the latest estimate from the Brazilian Institute of Geography and Statistics (IBGE), Paracatu has a current population of approximately 94.000 people (IBGE 2020).

2.2 Choice of the Analyzed Period, Acquisition and Standardization of Data

Images from the LANDSAT-5 and LANDSAT-8 satellites were obtained from the United States Geological Survey (USGS) website. Due to its temporal resolution, studies involving data from SR and space-time variation of the LST generally use a certain amount of images to represent a respective season of the year and even an entire year, according to related studies (Wang et al. 2018; Govind & Ramesh, 2019; Ahmadi et al. 2022).

However, studies that evaluate the real reason for LULC and its influence on a given parameter usually work with images of a single station (Carrasco et al. 2020), segmented stations (KHAN et al. 2023), or pairs of stations (Saha et al. 2024). However, the present study is distinguished by the fact that it presents images that represent the spatial distribution of all seasons of the year, in order to estimate the LST more accurately. However, it is worth noting that all images were recorded during the day. Thus, the LST reported here represents only the daytime period.

As a justification of the years chosen for analysis of the present study (1990 and 2020), we sought to analyze years in which it was possible to explore a period of time in which, in this interval, there was considerable urban expansion in the study area.

For the year 1990, it was not possible to work with images of the wet season (summer), therefore, it was decided to work with one more image of the autumn season, as it is a transition season in the study area (Santos et al. 2022b), between the period wet and dry, and also considering the influence of the presence/scarcity of water in the soil for the LST records, as its humidity tends to change the albedo and, as a result, the greater/lesser its ability to absorb and re-emitting energy (Sayão et al. 2020). The chosen dates are shown in Table 1. Table 2 shows the characteristics of the images.

At this point, it is worth pointing out that the quantitative description of the energy partition on the evaporating earth surfaces is extremely important to evaluate the earth-atmosphere exchange, especially for the interpretation of various Remote Sensing (RS) measurements, because the partitioning of the radioactive energy received on the evaporating (and drying) surfaces affects the heat exchange and mass transfer and, in turn, it defines the relationship between sensible and latent heat fluxes (Aminzadeh & Or 2014).

Laird and Kristovich (2002) and Tajfar et al. (2020) also highlight the issues of sensible and latent heat flux, emphasizing that these characterize the exchange of heat and moisture between the Earth's surface and its overlying atmosphere, and it is evident that their accurate estimation is of crucial importance for a better understanding of the processes of earth-atmosphere exchange.

Images were used in which there was no presence of clouds in the study area or that the scene was not composed of more than 10% of clouds, so as not to jeopardize the results obtained. In case of non-compliance with one of these premises, the scene would be discarded and another image would be chosen.

Finally, the Resampling and Resolution Reduction process was carried out, with the nearest neighbor technique, using the QGis 3.2.12 software (QGIS, 2021) to standardize all the pixels of the different satellites used (30 meters).

2.3 Extracting LST Estimation from Orbital Images

To calculate the LST estimated, the equation recommended by the USGS (2016) was applied. The Qgis 3.2.12 software (QGIS, 2019) was used in each image obtained and, using the raster calculator, the average, pixel by pixel, was performed between the 4 images in Table 1, in order to have an annual estimate of the average LST behavior for that period, based on images that characterize each season of the year.

Table 1 Dates of images used.

Year	Autumn	Winter	Spring	Summer
1990 (LANDSAT-5)	04-02; 05-20	08-08	09-16	*
2020 (LANDSAT-8)	05-22	07-09	09-27	03-19

* In view of the presence of clouds above the limit stipulated for this study for the summer season of 1990, in that year, it was decided to work with 2 images of the autumn season.

Table 2 Characteristics of the images used.

Scene data	Scene center time	Path/row	Cloud cover (%)	Band	Sensor	Spatial resolution (m)
08-08-1990	12:28:56	220/072	8.00	6	TM	30
09-16-1990	12:29:07	220/072	0.00	6	TM	30
05-20-1990	12:29:11	220/072	0.00	6	TM	30
02-04-1990	12:58:58	220/072	1.00	6	TM	30
05-22-2020	13:08:46	220/072	0.00	10	OLI	100
07-09-2020	13:08:46	220/072	0.00	10	OLI	100
09-27-2020	13:09:14	220/072	0.00	10	OLI	100
19-03-2020	13:08:45	220/072	5.63	10	OLI	100

The QGIS 3.30.1 SCP plugin was used to estimate the LST of LANDSAT thermal imaging. The process of recovery of the LST, in degrees Celsius, occurs as follows: conversion of the Digital Number (DN) values into radiance at the top of the atmosphere; conversion of radiance to brightness temperature at the top of the atmosphere; correction of atmospheric effects, obtaining surface temperature; and conversion of LST to Kelvin to degrees Celsius.

For the TM and OLI sensor bands, the radiance (Lλ) can be estimated based on Equation 1, which converts the DN (without unit of measurement) into the energy received at the top of the atmosphere (Watts/ (m² srad μm)). Subsequently, Equation 2 was applied to convert radiance into brightness temperature in the top of the atmosphere (ToA) and in Kelvin.

$$\text{(1)} \quad L\lambda = (M_L \text{ X } Q_{cal}) + A_L - O_i$$

Where Q_{cal} represents the image in DN; M_L indicates the specific multiplicative scale factor for the spectral band; A_L is an additive, bandwidth-specific scale factor accessed in the scene metadata.

$$\text{(2)} \quad T_B = \frac{K_2}{[\ln\left(\frac{k_1}{L_\lambda} + 1\right)]}$$

Where K_2 and K_1 are conversion constants for each thermal strip, being made available in the scene's metadata; L_λ is the radiance; T_b is the brightness temperature at the top of the atmosphere in Kelvin.

The emissivity values of the land surface (ε) (Equation 3) were estimated based on the values of the Normalized Difference Vegetation Index (NDVI). Thus, the following caveat was applied: a) in cases of NDVI lower than 0.2, the pixel is considered as bare soil, and emissivity is obtained from the reflective values in the red region; b) with NDVI greater than 0.5, the pixels are considered as vegetation and a constant value for emissivity (0.99) is assumed, and; c) NDVI between the 0.2 and 0.5 ranges, the pixel is composed of a mixture of bare soil and vegetation. This procedure was adopted based on the technical report made available by the National Aeronautics and Space Administration (NASA 2013), which presents the relationship between thermal emissivity and NDVI for natural surfaces, and it was verified that thermal emissivity was highly correlated with NDVI, with a correlation of R = 0.94. It is also worth noting that this step was estimated in the study by Sobrino et al. (2004), recommended by the USGS (2016) and explored by Parastatidis et al. (2017), which ratifies the use of emissivity based on NDVI, as the tests performed by the authors were very similar in terms of error with LST for urban areas, where land use is continually altered.

$$\text{(3)} \quad \varepsilon = \varepsilon_v P_v + \varepsilon_s (1 - P_v) + d_\varepsilon$$

Where εv and εs are, respectively, emissivity of vegetation and soil; Pv indicates the proportion of vegetation obtained by means of Equation 4.

$$\text{(4)} \quad P_v = \frac{NDVI - NDVI_{min}}{NDVI_{max} - NDVI_{min}}$$

Where $NDVI_{max}$ is equivalent to 0.5 and $NDVI_{min}$ describes the surface composed of the mixture of bare soil and vegetation (0.5). Source: Carlson and Ripley (1997); Sobrino et al. (2004).

To determine the term d_ε in Equation 3 it was assumed that this parameter is disregarded on smooth surfaces. For heterogeneous and rugged sites, such as vegetation, its value can reach 2%, as shown in Equation 5.

$$\text{(5)} \quad d_\varepsilon = (1 - \varepsilon_s)(1 - Pv) F_{\varepsilon_v}$$

Where F indicates a form factor and the average value is 0.55, assuming different geometric distributions.

The calculation of emissivity was performed based on Equation 6, and to calculate the values of m and n, Equations 7 and 8 were used, respectively.

$$\text{(6)} \quad \varepsilon = (m \; x \; P_v) + n$$

$$\text{(7)} \quad m = \varepsilon_v - \varepsilon_s - (1 - \varepsilon_s) F \varepsilon_v$$

$$\text{(8)} \quad n = \varepsilon_s + (1 - \varepsilon_s) F \varepsilon_v$$

Finally, it was possible to calculate the LST estimated in Kelvin using Equation 9.

$$\text{(9)} \quad T = \frac{T_B}{[1 + \left\{\frac{\lambda \text{ x } T_B}{\alpha}\right\} x \; Ln_\varepsilon}$$

Where λ is the central wavelength of the emitted radiation, with 11.5 μm being used for LANDSAT-5 band 6 and 10.8 μm for LANDSAT-8 band 10; α is the constant equal to 1.438 x 10^{-2} mK (Artis and Carnahan, 1982) and is calculated according to Equation 10.

(10) $$\alpha = h\,x\,\frac{C}{\sigma}$$

Where h is determined by Planck's constant ($6.626x10^{-34}$ Js); C corresponds to the speed of light (2.998 x 108 m/s); and σ is Boltzmann's constant ($1.38x10^{-23}$ J/K) (Weng et al. 2004).

It is noteworthy that the value of 273.15 was subtracted from the result obtained in Equation 9 to convert the Kelvin temperature into degrees Celsius. Regarding the calculation of the LST estimated of the LANDSAT-8 satellite, the value of –0.29 was added for each pixel of the resulting image of the average, as recommended by the USGS, since the thermal bands 10 and 11 receive interference from scattered light from areas adjacent to the imaged scene and therefore require this adjustment. The USGS recommends using band 10 during temperature estimation, as the stray light problem occurs, with greater intensity, in band 11 (USGS, 2016).

2.4 Extraction of Pixel Values from the Urban Grid and Data Analysis

A mask that represented the reality of the urban mesh of the municipality was used, which was obtained from the Planning Department of the municipality of Paracatu and with a scale of 1:50000.

After cutting the parameters for the area of interest, the files were exported to the ArcGis software (10.5) (ARCGIS 2022) to merge the attribute tables containing the results of the respective parameters, in order to analyze the possible impact of LULC on LST estimated over the years.

A layout was elaborated containing the LST estimated and the use and occupation of the study area during the years analyzed. In the LST layout, these images were separated into classes (quartiles), and their values were expressed in degrees Celsius and classified so that it was possible to visually verify the variation of the analyzed parameter over the years.

2.5 Single Mosaic from All Scenes for Estimation of Annual LST

In order to create a representative mosaic of all the scenes, the normalization process was carried out between each of them. This method was based on Lunetta (1995), developed for LANDSAT satellite scenes, and consists of equalizing the mean and variance values in both images, according to Equation 11.

(11) $$S' = \sqrt{\frac{\sigma^2 R}{\sigma^2 A}\,x\,S + \left(\mu R - \sqrt{\frac{\sigma^2 R}{\sigma^2 A}}\,x\,\mu A\right)}$$

Where: μR is the average between the reference images for each year (1990 and 2020) and μA is the average of the adjusted image. σR is the variance of the reference image and σA is the variance of the adjusted image. Lastly, S represents the image to be adjusted, while S' is the result of the adjusted image.

Finally, the average calculation of the 4 scenes to represent each year was performed and a mosaic was created in a GIS environment.

2.6 Obtaining, Extracting and Analyzing the LULC

The LULC rasters were downloaded for the chosen years, and later the study area mask was used to cut out the area of interest. In this study, the MapBiomas Level 6 classification was considered and the following classes of use and coverage were found for all periods: a) Forest Formation; b) Cerrado Formation; (c) Exposed Soil; d) Urban mesh; (e) Other Non-Vegetated Areas and; f) Water Resources.

MapBiomas is a collaborative and open-source monitoring initiative created in 2015 to fill in the information of LULC in Brazil, being innovative by acting in a network formed by ONGs, Universities and private companies organized by biomes and cross-cutting themes. It produces annually, through the Random Forest algorithm and for the entire national territory, via Earth Engine cloud computing, land use and occupation scenes (Azevedo et al. 2018).

Finally, by calculating the average of each year of the LST, the classes of use of MapBiomas were aggregated into 4, in order to reduce the number of classes and analyze their influence on the spatial variation of the LST, namely: a) urban mesh (which includes the pixels of the city of Paracatu); b) vegetation (includes pixels considered vegetative); c) water resources (pixels characterized as water) and; d) non-vegetated areas, which are those with exposed soil. Then, the data were cross-referenced in order to verify the variation of the spatial LST of each of these MapBiomas classes, as well as their area in each year analyzed, verifying their respective growth or decrease. Finally, a layout was elaborated containing the use and occupation in each year analyzed in a GIS environment.

3 Results

Figure 2 shows the map of spatial behavior of LST estimated for the years 1990 (A) and 2020 (B). Table 3 shows the maximum, average and minimum temperature variations for these periods based on the average of all scenes used for each year. The results of land use and occupation for the years 1990 (A) and 2020 (B) are presented in Figure 3, while the histogram containing the spatial behavior of the LST, based on the annual estimate, is shown in Figure 4.

Based on the results presented, it was possible to verify that the average LST estimated of the urban area of Paracatu increased by 2.56 ºC. Regarding its minimum temperature, there was a difference of 3.57 ºC and, in relation to the maximum, 2.47 ºC. The spectral behavior of pixels shows an increase in the urban area of the central surroundings of the city, moving away from the center over the years, which is a result of the urbanization process.

It is worth noting that Santos and Simionatto (2023), when evaluating the places with potential formation of UHI in the city of Paracatu, concluded that, for an interval of 14 years, the neighborhoods most prone to the occurrence of the phenomenon tripled, from 4 to 12, pointing to a need to mitigate the impacts caused by urban expansion, especially with the support of public agencies for the insertion of green areas in the city.

Another factor to be considered and related to the results of LST/LULC variation found is the exponential increase in the cost of housing in the city, especially after the arrival of the medical school and the sale of the open-pit mining (gold) activity to a Canadian company, becoming one of the most important multinationals in Latin America in this regard. These situations, as much as they heat up the local economy and increase the floating population, have a direct impact on the real estate sector, inflating property values and making these new residents look for more distant places to live, which is visually verified when analyzing the variation of LULC in the city of Paracatu.

It is worth mentioning that, in view of these results, there is an elimination of vegetation in practically the entire territory of the city, a fact that is related to urban expansion and the scenario mentioned above. In addition, the LULC of a specific neighborhood (Bom Pastor) stands out, which in 1990 was completely covered by vegetation. On the other hand, in 2020, the entire neighborhood became urbanized and without mitigating measures to contain the impacts caused by the suppression of vegetation and the increase in impermeable areas. Table 4 shows the average, minimum, and maximum behavior of this neighborhood based on the annual estimate represented by the average of the images for the years 1990 and 2020.

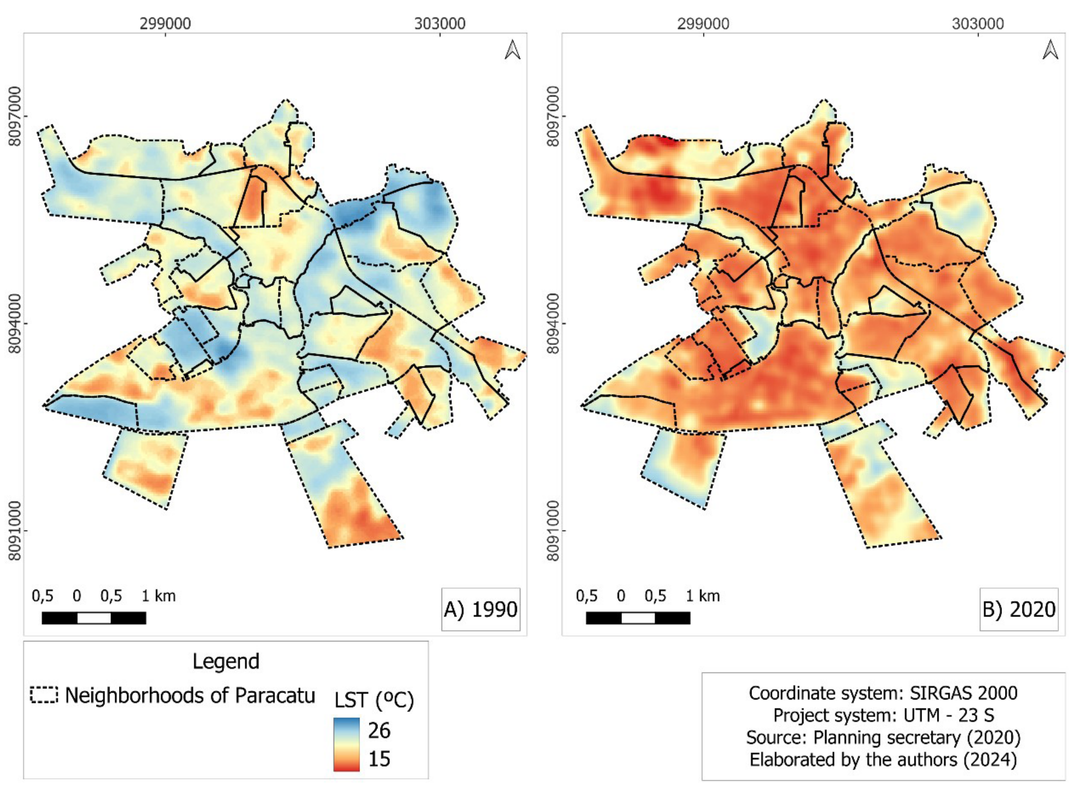

Figure 2 LST estimated, during the analyzed period, in the study area.

Table 3 Average, maximum and minimum LST values.

	Minimum (ºC)*	Maximum (ºC)*	Average (ºC)*
1990	15.96	23.33	20.42
2020	19.53	25.80	22.98

* Minimum, mean and maximum LST values extracted based on the averages of the images used for each year in order to estimate the spectral behavior of the year.

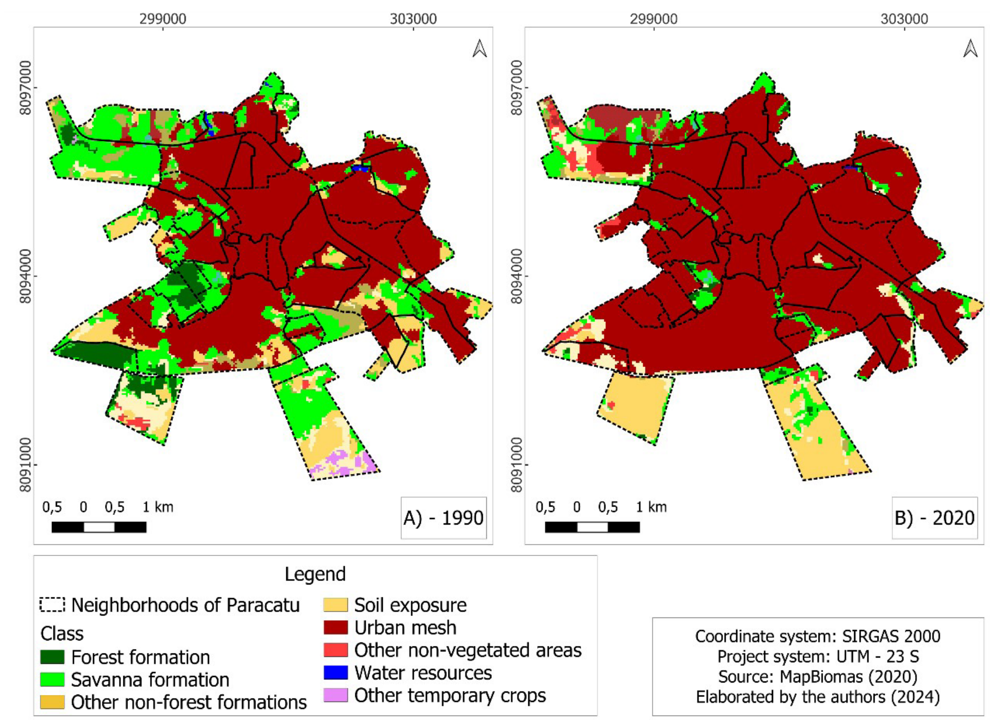

Figure 3 Land use and occupation of Paracatu in: A. 1990; B. 2020.

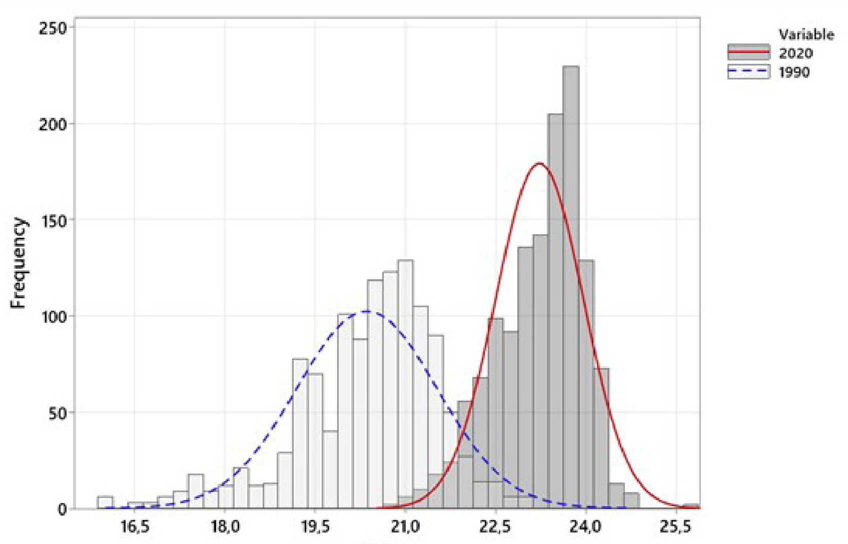

Figure 4 Histogram of the LST estimative of the city of Paracatu for the years 1990 and 2020 based on the average of the scenes used to represent the year 1990 (LANDSAT-5) and 2020 (LANDSAT-8).

Table 4 Variation of the LST in the Bom Pastor neighborhood.

	1990	2020
Average (ºC)	18.67	23.89
Minimum (ºC)	17.82	23.47
Maximum (ºC)	20.71	24.34

It is noted that there was an increase of more than 5º in the average LST estimated of this neighborhood, in addition to a significant increase in its minimum and maximum. It is noteworthy that this value was found based on the average of the 4 images used to estimate and represent the behavior of this parameter for the year. Therefore, it is possible to infer that the suppression of vegetation, especially in this neighborhood, is closely related to the variation in the behavior of the LST, given the correlation of these parameters, as presented by Santos et al. (2023), who verified, in the watershed that supplies the city of Paracatu, the impact caused by the LULC on the variation of the LST. Santos et al. (2022a) also verified the impact caused by the suppression of vegetation in the open-pit mining area in Paracatu, finding correlations with the variation of LST.

The mean evolution of the LST estimated of each occupational class is shown in Figure 5 and Table 5 shows the area of each class analyzed in the respective years. As there was no presence of water resources in 2020, this class was disregarded from this analysis. Table 6 presents the minimum and maximum values of the LST estimate for each class of use and occupation evaluated.

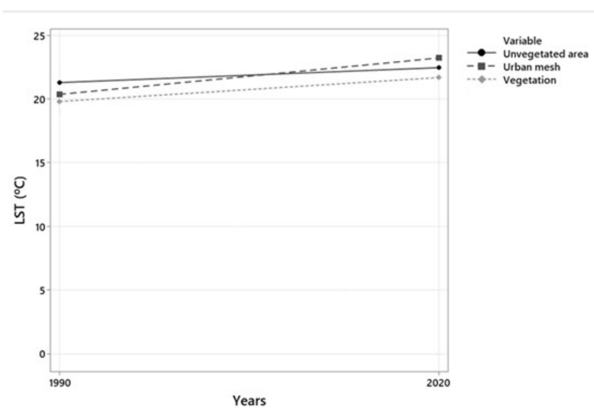

Figure 5 LST estimated evolution in each occupation class.

Initially, it should be noted that the difference between the total area of the classes is due to the junction between the macroclasses of MapBiomas, so that pre-existing classes in 1990 were not considered in the junction for the analysis of the junction between them.

The results show that the classes of vegetation, exposed soil and urban mesh showed an average spatial increase of LST, which is closely related to the process of urban expansion in the city of Paracatu. In addition, the class of water resources was not computed for the year 2020, which points to a need to protect the streams and rivers that enter the city, but which, for resolution reasons, were not captured by the 30-meter resolution used by MapBiomas. However, as they are results validated by an agency that aims to monitor changes in the territory, it is possible to infer that there was a decrease in the water class in the urban mesh.

It is also important to highlight the expansion of the city and the reduction of the plant class, since, while the urban area doubled its territorial extension, increasing by 418.5 km², the vegetative class decreased by 204.3 km². Therefore, it is possible to induce that the expansion that occurred in the municipality, linked to the suppression of vegetation, is directly related to the spatial variation of the LST estimated, directly impacting the public health of the population of Paracatu, as addressed by Macintyre et al. (2018), who predict that urbanization and climate change will directly increase the incidence of health risks related to UHIs.

From this perspective, it is worth mentioning that an efficient urban management that is capable of solving such problems is increasingly a challenge for public agencies that manage and supervise, because the negative impacts from LULC, especially on LST, represent a series of threats to the biogeochemical and biophysical processes of the ecosystem (Shen et al. 2022).

In addition, the results show that, in 1990, Paracatu was basically composed of built area and vegetation. 30 years later, the city is, above all, composed of impermeable areas, while the vegetative class is only not less than the class of water resources, pointing to a need for urban and environmental management, linked to the pillars of economic development, so that urban expansion can occur, but with strategic points distributed throughout the new extensions. in order to mitigate the negative impacts arising from this transformation, a fact that, until 2020, did not occur in the city of Paracatu.

Table 5 Area (km²), in 1990 and 2020, of the analyzed classes.

	1990 (km²)	2020 (km²)	1990 (%)	2020 (%)
Vegetation	300.6	96.3	33.81	8.86
Exposed soil	168.3	154.8	18.93	14.24
Urban mesh	417.6	836.1	46.96	76.90

Table 6 Minimum and maximum LST values in each class of use and occupancy.

1990	Vegetation	Exposed soil	Urban mesh
Minimum (ºC)	15.96	18.12	16.38
Maximum (ºC)	20.19	23.33	22.95
2020	Vegetation	Exposed soil	Urban mesh
Minimum (ºC)	19.53	20.19	20.82
Maximum (ºC)	23.50	23.90	25.80

*Values not found for the class that year.

Finally, the results of the variations of the minimum and maximum LST estimated in each LULC class indicate the influence of vegetation suppression for the increase of the built area in the LST variation, especially in the case of the minimum pixel value in the urban area and vegetation classes, which increased by almost 4.5 ºC. with a variation of 3 ºC was found for the maximum LST values.

The increase in the LST value of the pixels of each class is related to urban climate definitions (Williams 1991), in which the suppression of vegetation to increase impervious areas alters the microclimate at the "microscale" of the underlying land surface (Yang et al. 2023).

In this context, Rezende (2016) found that the new residential occupations in the municipality are lacking in vegetation on the sidewalks, which should not occur, since, since 2009, the executive branch has made it mandatory to plant trees on public sidewalks, respecting pedestrian traffic in new buildings, and planting and conservation are the responsibility of the landowner. As much as the public administration fulfills its role of requiring the planting of trees on the sidewalks, this is not strictly complied with by the residents, who plant them only to get the power to occupy the property.

Finally, in view of the scarcity of the vegetation class and the exponential increase in impermeable areas without the necessary mitigation measures to ensure the quality of public health for citizens, it is essential that these are implemented by public agencies, such as, for example, reforestation and the implementation of parks in the neighborhoods most impacted by urban expansion. based on the results presented by the present study, since these measures can reduce the impacts of local climate change and UHI phenomena.

4 Conclusion

The results obtained show that the city of Paracatu showed exponential growth in its built area between the years 1990 and 2020, while the classes that represent the natural environment showed a significant decrease, with emphasis on vegetation, which went from 300.6 km² to 96.3 km².

On the other hand, in 2020, the urban area was twice as large as its area in 1990, and it is possible to conclude that these changes directly impacted the variation of the minimum, average and maximum LST of the city, with emphasis on the average increase of approximately 5º C, a fact that directly and negatively impacts the public health of citizens. Esse cenário também foi verificado ao analisar as variações mínimas e máximas de LST em cada classe, apontando para uma alteração do microclima da cidade.

It is noteworthy that the results presented here represent only an estimate of the behavior of the LST for this period, and that due to the limitations of the temporal analysis of the LANDSAT satellite, these indications represent only the behavior of this parameter in the daytime period, which is a limitation of the study, which is also restricted to the number of scenes used to represent each period.

In this aspect, it is believed that there are future perspectives of analysis, involving more scenes of each year and also the behavior of LST in other periods of the day through the use of another satellite, in order to investigate, in depth, the microclimate of the city of Paracatu.

Finally, it is believed that the method of analysis of the variation of LULC and LST used in this study can subsidize the public power for territorial management purposes, in order to implement strategic areas that can mitigate the negative impacts caused by thermal variation in the city.

5 References

Ahmadi, S., Alizadeh, H., & Mojaradi, B. 2022, Land surface temperature assimilation into a soil moisture-temperature model for retrieving farm-scale root zone soil moisture, *Geoderma*, vol. 421, no. 115923, pp. 1-18. viewed 03 october 2022, <https://doi.org/10.1016/j.geoderma.2022.115923>.

Aminzadeh, M., & Dani, O. 2014, Energy partitioning dynamics of drying terrestrial surfaces, *Journal of hydrology*, vol. 519, pp. 1257-1270, viewed 03 october 2022, <https://doi.org/10.1016/j.jhydrol.2014.08.037>.

ARCGIS – ARC Geographic Information System 2022, *ArcGis*: Software, viewed 03 october 2022, <https://www.esri.com/software/arcgis/index.html>.

Artis, D.A., & Carnahan, W.H. 1982. Survey of emissivity variability in thermography of urban areas. *Remote Sens Environ*, vol. 12, pp. 313-329, viewed 03 october 2022, <https://doi.org/10.1016/0034-4257(82)90043-8>.

Azevedo, S.R., Souza, C.M., Shimbo, J., & Alencar, A. 2018. MapBiomas initiative: Mapping annual land cover and land use changes in Brazil from 1985 to 2017, *AGU Fall Meeting Abstracts*, vol. 2018, pp. B22A-04, viewed 03 october 2022, <https://ui.adsabs.harvard.edu/abs/2018AGUFM.B22A..04A/abstract>.

Carlson, T.N., & Ripley, D.A. 1997, On the relation between NDVI, fractional vegetation cover, and leaf area index, *Remote Sens Environ*, vol. 62, pp. 241-252, viewed 03 october 2022, <https://doi.org/10.1016/S0034-4257(97)00104-1>.

Carrasco, R.A., Pinheiro, M.M.F., Marcato JR, J., Cicerelli, R.E., Silva, P.A., Osco, L.P., & Ramos, A.P.M. 2020, Land use/land cover change dynamics and their effects on land surface temperature in the western region of the state of São Paulo, Brazil, *Regional Environmental Change*, vol. 20, no. 96, viewed 03 october 2022, <https://doi.org/10.1007/s10113-020-01664-z>.

Govind, N., & Ramesh, H. 2019, The impact of spatiotemporal patterns of land use land cover and land surface temperature on an urban cool island: A case study of Bengaluru, *Environmental monitoring and assessment*, vol. 191, pp. 1-20. viewed 03 october 2022, <https://link.springer.com/article/10.1007/s10661-019-7440-1>.

IBGE – Instituto Brasileiro de Geografia e Estatística 2020, *Produto Interno Bruto dos Municípios*. Paracatu – MG, viewed 03 october 2022, <https://www.ibge.gov.br/estatisticas>.

IBGE – Instituto Brasileiro de Geografia e Estatistica 2020, *Censo demográfico 1991*, viewed 03 january 2024, <https://www.ibge.gov.br/estatisticas/sociais/trabalho/25089-censo-1991-6.html?edicao=25090>.

IBGE – Instituto Brasileiro de Geografia e Estatistica 2020, *Censo demográfico 2022*, viewed 03 january 2024, <https://www.ibge.gov.br/estatisticas/sociais/trabalho/22827-censo-demografico-2022.html>.

IBGE – Instituto Brasileiro de Geografia e Estatistica 2020, *Estimativas* populacionais, viewed 03 january 2024, <https://www.ibge.gov.br/cidades-e-estados/mg/paracatu.html>.

INMET – Instituto Nacional de Meteorologia 2020, *Normais climatológicas do Brasil*, viewed 03 october 2022, <https://portal.inmet.gov.br/normais>.

Ismail, M. H., Aik, D. H. J., Alias, M. A., Muharam, F. M., & Zaki, P. H. 2021, Land Use/Land Cover (LULC) Changes in Cameron Highlands, Malaysia: Explore the Impact of the LULC Changes on Land Surface Temperature (LST) Using Remote Sensing, *Climate Impacts on Sustainable Natural Resource Management*, vol. 14, pp. 279-301, viewed 03 october 2022, <https://doi.org/10.1002/9781119793403.ch14>.

Jiang, L., & O'Neill, B.C., 2017, Global urbanization projections for the shared socioeconomic pathways Global Environ, *Global Environ. Change*, vol. 42, pp. 193-199, viewed 03 october 2022, <https://doi.org/10.1016/j.gloenvcha.2015.03.008>.

Kafy, A., Saha, M., Fisal, A., Rahaman, Z.A., Rahman, M.T., Lui, D., Fattah, M.A., Rakib, A.A., AlDousari, A.E., Rahaman, S.N., Hasan, M.Z., & Ahasan, M.A.K. 2022, Predicting the impacts of land use/land cover changes on seasonal urban thermal characteristics using machine learning algorithms, *Building and Environment*, vol. 217, no. 109066, viewed 03 october 2022, <https://doi.org/10.1016/j.buildenv.2022.109066>.

Khan, M., Qasim, M., Tahir, A.A., & Farooqi, A. 2023, Machine learning-based assessment and simulation of land use modification effects on seasonal and annual land surface temperature variations, *Heliyon*, vol. 9, n. 12, pp. e23043, viewed 03 october 2022, <https://doi.org/10.1016/j.heliyon.2023.e23043>.

Laird, N.F., Kristovich, D.A.R. 2002, Variations of sensible and latent heat fluxes from a Great Lakes buoy and associated synoptic weather patterns, *Journal of Hydrometeorology*, vol. 3, no. 1, pp. 3-12, viewed 03 october 2022, <https://doi.org/10.1175/1525-7541(2002)003%3C0003:VOSALH%3E2.0.CO;2>.

Lopes, H.S., Remoaldo, P.C., Ribeiro, V., & Martin-Vide, J. 2022, Análise do ambiente térmico urbano e áreas potencialmente expostas ao calor extremo no município do Porto (Portugal), *Cuadernos de Geografía: Revista Colombiana de Geografía*, vol. 31, no. 2, viewed 03 october 2022, <https://doi.org/10.15446/rcdg.v31n2.91309>.

Lunetta, R.S. 1995, Relative radiometric normalization of (MSS) Landsat multispectral scanner (MSS) data using an automatic scattergram-controlled regression, *Photogramm Eng Remote Sens*, vol. 10, no. 1, pp. 1255-1260, viewed 03 october 2022,

<https://www.asprs.org/wp-content/uploads/pers/1995journal/oct/1995_oct_1255-1260.pdf>.

Macintyre, H.L., Heaviside, C., Taylor, J., Picetti, R., Symonds, P., Cai, X.M., & Vardoulakis, S. 2018, Assessing urban population vulnerability and environmental risks across an urban area during heatwaves–Implications for health protection. *Science of the Total Environment*, vol. 610, pp. 678-690, viewed 03 october 2022, <https://doi.org/10.1016/j.scitotenv.2017.08.062>.

Monteiro, C.A.F. 1997, *Teoria e Clima Urbano*, IGEOG/USP (Série Teses e Monografias, 25), São Paulo.

Nagendra, H., Bai, X., Brondizio, E.S., & Lwasa, S. 2018, The urban south and the predicament of global sustainability, *Nature Sustainability*, vol. 1, pp. 341-349, viewed 03 october 2022, <https://doi.org/10.1038/s41893-018-0101-5>.

NASA - National Aeronautics and Space Administration 2013. *NTRS - NASA Technical Reports Server*. On the relationship between thermal emissivity and the Normalized Difference Vegetation Index for natural surfaces, viewed 10 may 2024, <https://ntrs.nasa.gov/citations/19930062068>.

ONU – Organização das Nações Unidas 2019, *World urbanization prospects 2018*: Highlights, viewed 03 october 2022, <https://population.un.org/wup/publications/Files/WUP2018-Highlights.pdf>.

Parastatidis, D., Mitraka, Z., Chrysoulakis, N., & Abrams, M. 2017, Online global land surface temperature estimation from Landsat, *Remote Sensing,* vol. 9, no. 12, 1208, viewed 03 october 2022, <https://doi.org/10.3390/rs9121208>.

QGIS – Q Geographic Information System 2019, *Open Source Geospatial Foundation Project*, viewed 03 october 2022, <https://www.qgis.org/it/site/>.

QGIS – Q Geographic Information System 2021, *Open Source Geospatial Foundation Project*, viewed 03 october 2022, <https://www.qgis.org>.

Rezende, P.S. 2016, Metodologia para avaliação da vulnerabilidade socioambiental: estudo da cidade de Paracatu (MG). 194 f. Dissertação (Mestrado em Ciências Humanas) - Universidade Federal de Uberlândia, Uberlândia, http://doi.org/10.14393/ufu.di.2016.49

Saha, S., Saha, A., Das, M., Saha, A., Sarkar, R., & Das, A. 2021, Analyzing spatial relationship between land use/land cover (LULC) and land surface temperature (LST) of three urban agglomerations (UAs) of Eastern India, *Remote Sensing Applications: Society and Environment*, vol. 22, no. e100507, viewed 03 october 2022, <https://doi.org/10.1016/j.rsase.2021.100507>.

Saha, J., Ria, S.S., Sultana, J., Shima, U.A., Seyan, M.M.H., Rahman, M.M. 2024, Assessing seasonal dynamics of land surface temperature (LST) and land use land cover (LULC) in Bhairab, Kishoreganj, Bangladesh: A geospatial analysis from 2008 to 2023. *Case Studies in Chemical and Environmental Engineering*, vol. 9, e100560, viewed 03 october 2022, <https://doi.org/10.1016/j.cscee.2023.100560>.

Santos, A.P., Santil, F.L.P., Carbone, S., & Silva, C.R. 2022a. The influence of urban and mineral expansion on surface temperature variation, *Acta Scientiarum*, Technology, vol. 45, n.1, e60114, viewed 03 october 2022, <https://doi.org/10.4025/actascitechnol.v45i1.60117>.

Santos, A., Santil, F., Oliveira, P., & Roveda, J. 2021. Utilização da Lógica Fuzzy como suporte ao Zoneamento Ambiental: um estudo de caso em Paracatu – MG. *Revista Brasileira De Geografia Física*, vol. 14, no. 4, pp. 2352-2368, viewed 03 october 2022, <https://doi.org/10.26848/rbgf.v14.4.p2352-2368>.

Santos, A., & Simionatto, H. 2023. Methodological proposal for evaluating the transformation of urban microclimate in medium-sized cities: A case study in the urban mesh of the municipality of Paracatu, Minas Gerais. *RAEGA* - O Espaço Geográfico em Análise, vol. 57, pp. 46-65, viewed 03 october 2022, <https://doi.org/10.5380/raega.v57i0.88156>.

Santos, A.P., Simionatto, H.H., Arantes, L.T., Simonetti, V.C., Oliveira, R.A., Sales, J.C.A., & Silva, D.C.C. 2023, The Influence of Land Use and Land Cover on Surface Temperature in a Water Catchment Sub-Basin, *Sociedade & Natureza*, vol. 35, no. 1, viewed 03 october 2022, <https://doi.org/10.14393/SN-v35-2023-69161>.

Santos, A.P., Simionatto, H.H., & Xisto, L.A.D. 2022b, Técnicas de PDI Aplicadas Para a Identificação e Extração Automática de Atividades Antrópicas, *Revista Brasileira De Geografia Física*, vol. 15, no. 4, pp. 2121-2137, viewed 03 october 2022, <https://doi.org/10.26848/rbgf.v15.4.p2121-2137>.

Sayão, V.M., Santos, N.V., Mendes, W.S., Marques, K.P.P., Safanelli, J.L., Poppiel, R.R., & Demattê, J.A.M. 2020, Land use/land cover changes and bare soil surface temperature monitoring in southeast Brazil, *Geoderma Regional*, vol. 22, e00313, viewed 03 october 2022, <https://doi.org/10.1016/j.geodrs.2020.e00313>.

Shen, X., Liu, Y., Liu, B., Zhang, J., Wang, L., Lu, X., & Jiang, M. 2022. Effect of shrub encroachment on land surface temperature in semi-arid areas of temperate regions of the Northern Hemisphere, *Agricultural and Forest Meteorology*, vol. 320, e108943, viewed 03 october 2022, <https://doi.org/10.1016/j.agrformet.2022.108943>.

Sobrino, J.A., Jiménez-Muñoz, J.C., & Paolini, L. 2004, Land surface temperature retrieval from LANDSAT TM 5, *Remote Sens Environ*, vol. 90, pp. 434-440, viewed 03 october 2022, <https://doi.org/10.1016/j.rse.2004.02.003>.

Sresto, M.A., Siddika, S., Fattah, M.A., Morshed, S.R., & Morshed, M.M. 2022, A GIS and remote sensing approach for measuring summer-winter variation of land use and land cover indices and surface temperature in Dhaka district, Bangladesh, *Heliyon*, vol. 8, e10309, viewed 03 october 2022, <https://doi.org/10.1016/j.heliyon.2022.e10309>.

Steeneveld, G., Klompmaker, J.O., Groen, R.J.A., & Holtslag, A.A.M. 2018, An urban climate assessment and management tool for combined heat and air quality judgements at neighbourhood scales, *Resources, Conservation and Recycling*, vol. 132, pp. 204-217, viewed 03 october 2022, <https://doi.org/10.1016/j.resconrec.2016.12.002>.

Tajfar, E., Bateni, S.M., Lakshmi, V., & Ek, M. 2020, Estimation of surface heat fluxes via variational assimilation of land surface temperature, air temperature and specific humidity into a coupled land surface-atmospheric boundary layer model, *Journal of Hydrology*, vol. 583, e124577, viewed 03 october 2022, <https://doi.org/10.1016/j.jhydrol.2020.124577>.

USGS – United States Geological Survey 2016, *Earth Explorer*, viewed 03 october 2022, <https://earthexplorer.usgs.gov/>.

Vandamme, S., Demuzere, M., Verdonck, M., Zhang, Z., & Coillie, F.V. 2019, Revealing kunming's (china) historical urban planning policies through local climate zones, *Remote Sensing*, vol. 11, no. 14, e1731, viewed 03 october 2022, <https://doi.org/10.3390/rs11141731>.

Wang, Y.C., Hu, B.K.H., Myint, S.W., Feng, C.C., Chow, W.T.L., Passy, P.F. 2018, Patterns of land change and their potential impacts on land surface temperature change in Yangon, Myanmar, *Sci Total Environ*, vol. 643, pp. 738-750, viewed 03 october 2022, <https://doi.org/10.1016/j.scitotenv.2018.06.209>.

Weng, Q., Lu, D., & Schubring, J. 2004. Estimation of land surface temperature vegetation abundance relationship for urban heat island studies, *Remote Sens Environ*, vol. 89, pp. 467-448, viewed 03 october 2022, <https://doi.org/10.1016/j.rse.2003.11.005>.

Williams, T.B. 1991, Microclimatic temperature relationships over different surfaces, *Journal of Geography*, vol. 90, no. 6, pp. 285-291, viewed 03 october 2022, <https://doi.org/10.1080/00221349108979321>.

Yang, S., Wang, L., Stathopoulos, T., & Marey, A.M. 2023. Urban microclimate and its impact on built environment – A review, *Building and Environment*, vol, 238, e110334, viewed 03 october 2022, <https://doi.org/10.1016/j.buildenv.2023.110334>.

Zago, N. 2016, Migração rural-urbana, juventude e ensino superior, *Revista Brasileira de Educação*, vol. 21, pp. 61-78, viewed 03 october 2022, <https://doi.org/10.1590/S1413-24782016216404>.

Zhang, W., Li, Y., Li, Z., Wei, X., Ren, T., Liu, J., & Zhu, Y. 2020, Impacts of climate change, population growth, and urbanization on future population exposure to long-term temperature change during the warm season in China, *Environmental Science and Pollution Research,* vol. 27, pp. 8481-8491, viewed 03 october 2022, <https://doi.org/10.1007/s11356-019-07238-9>.

Author contributions
Arthur Pereira dos Santos: conceptualization; data collection and processing; discussion; writing-original draft; writing – review; supervision. Henzo Henrique Simionatto: conceptualization; data collection and processing; discussion; writing-original draft; writing – review and editing.

Conflict of interest
The authors declare no conflict of interest.

Data availability statement
All data included in this study are publicly available in the literature.

Funding information
Not applicable.

Editor-in-chief
Dr. Claudine Dereczynski

Associate Editor
Dr. Gerson Cardoso da Silva Jr.

How to cite:

Santos, A.P. & Simionatto, H. H. 2024, 'Spatial Analysis of the Impacts Caused by Changes in Land Use on the Estimation of Surface Temperature in the The City of Paracatu (MG)'